Structure of an Hsp90-Cdc37-Cdk4 complex

Article (Published Version)

Molecular Cell *23*, 697–707, September 1, 2006 ©2006 Elsevier Inc. DOI 10.1016/j.molcel.2006.07.016

Structure of an Hsp90-Cdc37-Cdk4 Complex

Cara K. Vaughan,[1] Ulrich Gohlke,[2,4] Frank Sobott,[3,5] Valerie M. Good,[1] Maruf M.U. Ali,[1] Chrisostomos Prodromou,[1] Carol V. Robinson,[3] Helen R. Saibil,[2] and Laurence H. Pearl[1,*]

[1] Section of Structural Biology
The Institute of Cancer Research
Chester Beatty Laboratories
237 Fulham Road
London SW3 6JB

[2] Department of Crystallography
Birkbeck College
Malet Street
London WC1E 7HX

[3] Cambridge University Chemical Laboratory
University of Cambridge
Lensfield Road
Cambridge CB2 1EW
United Kingdom

Summary

Activation of many protein kinases depends on their interaction with the Hsp90 molecular chaperone system. Recruitment of protein kinase clients to the Hsp90 chaperone system is mediated by the cochaperone adaptor protein Cdc37, which acts as a scaffold, simultaneously binding protein kinases and Hsp90. We have now expressed and purified an Hsp90-Cdc37-Cdk4 complex, defined its stoichiometry, and determined its 3D structure by single-particle electron microscopy. Comparison with the crystal structure of Hsp90 allows us to identify the locations of Cdc37 and Cdk4 in the complex and suggests a mechanism by which conformational changes in the kinase are coupled to the Hsp90 ATPase cycle.

Introduction

Association with the Hsp90 molecular chaperone system is an essential prerequisite for activation of an important set of protein kinases in the eukaryotic cell. The list of Hsp90's kinase "clientele" includes key regulators such as PKB/Akt (Basso et al., 2002; Fontana et al., 2002; Sato et al., 2000), PDK1 (Fujita et al., 2002), LKB1 (Boudeau et al., 2003), Raf-1 (Grammatikakis et al., 1999; Schulte et al., 1995; Stancato et al., 1993), ErbB2 (Xu et al., 2001), Src-family kinases (Bijlmakers and Marsh, 2000; Xu and Lindquist, 1993; Xu et al., 1999), Aurora B (Lange et al., 2002), RIP (Lewis et al., 2000), components of the IκB kinase complex (Chen et al., 2002), and the cyclin-dependent kinases Cdk4, Cdk6, and Cdk9 (Mahony et al., 1998; O'Keeffe et al., 2000; Stepanova et al., 1996). In all cases analyzed, the Hsp90-dependent activation of the kinase is found to be dependent on the ATPase cycle of the chaperone (Prodromou et al., 2000) so that pharmacological inhibition by Hsp90 binding ATP competitors (Prodromou et al., 1997; Roe et al., 1999; Stebbins et al., 1997) prevents client activation. As disregulation of many of these kinases is directly implicated in development and progression of cancer (Workman, 2004), understanding the molecular basis for kinase activation by Hsp90 is key to the development of new cancer chemotherapies.

Recruitment of kinases to Hsp90 depends on Cdc37 (also known as $p50^{cdc37}$), originally discovered as a component of an Hsp90 complex with the viral oncogene v-Src (Brugge, 1986). Subsequently, Cdc37 has been found associated with essentially all protein kinases whose activation is Hsp90 dependent (Pearl, 2005), including the cyclin-dependent kinase Cdk4 (Dai et al., 1996; Lamphere et al., 1997; Stepanova et al., 1996). Overexpression of Cdc37 is itself oncogenic, reflecting its association with many pro-oncogenic kinases and suggesting that their Cdc37-dependent recruitment to the Hsp90 system may be limiting to their transforming potential (Stepanova et al., 2000a, 2000b). Cdc37 acts as a protein kinase-specific adaptor, recruiting client protein kinases to the Hsp90 system (Silverstein et al., 1998). Interaction of Cdc37 with protein kinases is mediated by the N-terminal segment (Grammatikakis et al., 1999; Shao et al., 2003a), while the middle and C-terminal regions of Cdc37 mediate interaction with Hsp90 (Roe et al., 2004; Shao et al., 2001; Zhang et al., 2004).

As with some other Hsp90 cochaperones, Cdc37 regulates the conformationally coupled ATPase mechanism of Hsp90, arresting the chaperone cycle in the client-loading phase, prior to Hsp90's ATP-dependent N-terminal dimerization (Siligardi et al., 2002; Roe et al., 2004). Cdc37 binds to the "lid" segment in the N-terminal domain of Hsp90, preventing its closure over the nucleotide binding site and locking the N-terminal domains of the chaperone apart. This prevents the formation of the N-terminally dimerized "tense" conformation of Hsp90 engendered by ATP binding (Chadli et al., 2000; Prodromou et al., 2000). Considerably less well understood is the basis of Cdc37's specific and selective binding to protein kinase clients. Minimally, the intact N-terminal lobe of the kinase is required for interaction with Cdc37 (Prince and Matts, 2004; Scroggins et al., 2003) and the conserved glycine-rich loop plays a role in the interaction (Zhao et al., 2004). However, this feature is present in many protein kinases that are not Hsp90 clients and does not explain the high specificity of Cdc37. Similarly, the location of the interaction between the client kinase and Hsp90 itself in a Cdc37-scaffolded complex is also poorly described. Mutagenesis studies suggest involvement of residues in the middle segment of the chaperone (Basso et al., 2002; Fontana et al., 2002; Meyer et al., 2003; Sato et al., 2000), but the nature of the interaction and how Hsp90 association activates the bound kinase remains obscure.

Key to understanding the Hsp90/Cdc37-dependent activation of protein kinase clients is the ability to study

*Correspondence: laurence.pearl@icr.ac.uk
[4] Present address: PSF Biotech AG, Heubnerweg 6, 14059 Berlin, Germany.
[5] Present address: Structural Genomics Consortium, University of Oxford, Botnar Research Centre, Oxford OX3 7LD, United Kingdom.

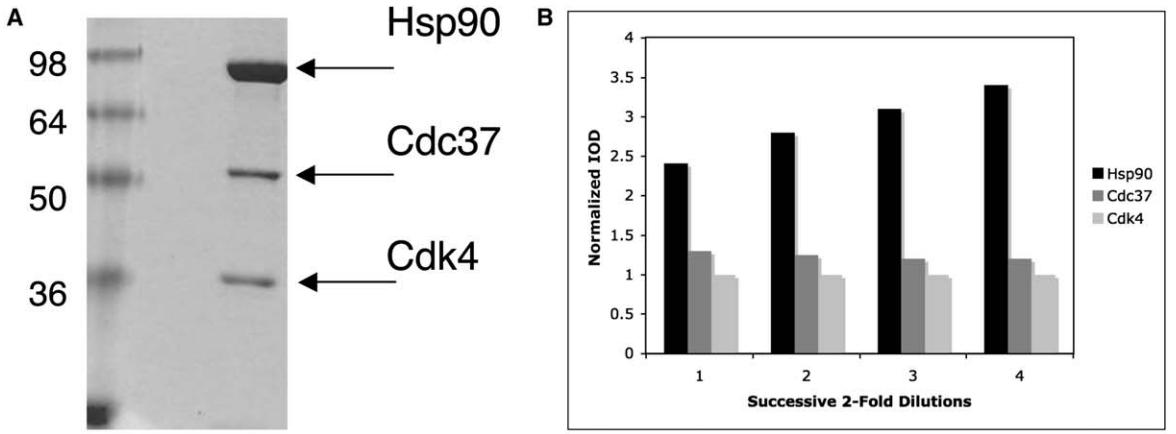

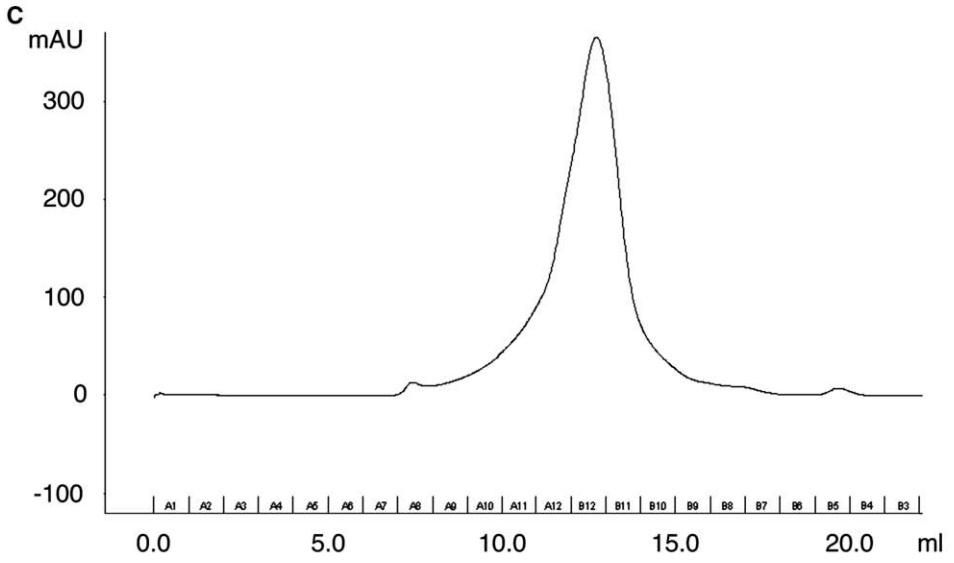

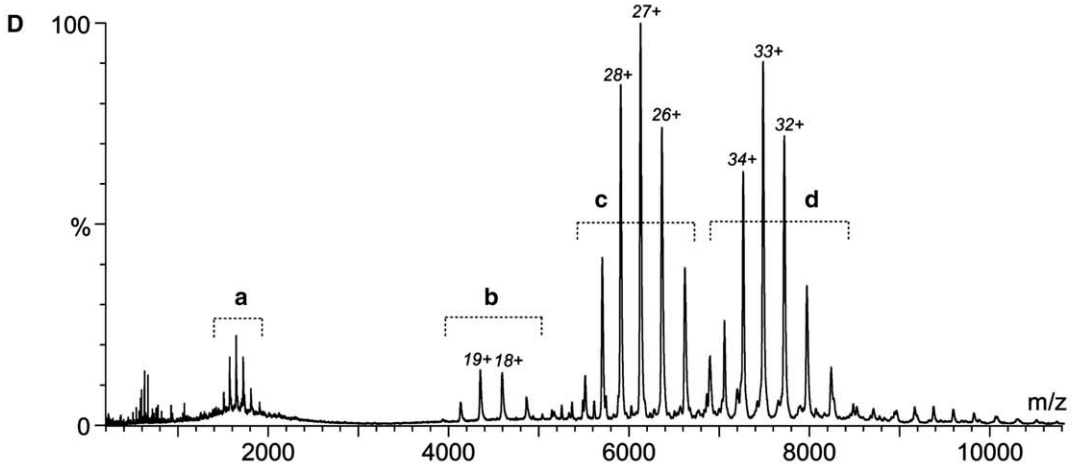

E

Peak series	Measured mass	Species
A	36 173 ±12 Da	Cdk4
B	82 721 ±14 Da	Hsp90
C	165 488 ±44 Da	$(Hsp90)_2$
D	247 113 ±83 Da	$(Hsp90)_2$-Cdc37-Cdk4

the structure and biochemistry of defined complexes in vitro. We have developed a recombinant system that allows production of assembled ternary Hsp90-Cdc37-kinase complexes at a milligram level. Using this, we have purified an Hsp90-Cdc37-Cdk4 complex to homogeneity, defined its stoichiometry, and determined its 3D structure by single-particle reconstruction from negative-stain electron microscopy (EM). Comparison with the crystal structure of an Hsp90 dimer in the ATP bound conformation (Ali et al., 2006) allows the identification of the chaperone domains and the location of Cdc37 and Cdk4 in the complex, providing the first structural view of client protein bound to the Hsp90 molecular chaperone and suggesting a mechanism for coupling the Hsp90 ATPase cycle to conformational changes in bound client protein kinases.

Results

Isolation and Compositional Analysis of Hsp90-Cdc37-Protein Kinase Complex

Recombinant expression of Hsp90, Cdc37, and several protein kinase clients in isolation has been reported previously by ourselves and others. However, assembly of well-behaved and stoichiometric Hsp90-Cdc37-kinase complexes by mixing purified proteins in vitro has proven refractory, suggesting that other cellular factors are probably involved in the client-loading process. We sought to bypass this problem by coexpressing components using a baculovirus vector in *Sf9* cells (see Experimental Procedures). Using this system, we could express His_6-tagged human Cdk4 and human B-Raf catalytic domain at useful levels, in the presence of coexpressed human Cdc37. Fractionation of cell lysates by using immobilized metal affinity chromatography (IMAC) yielded coeluting Cdk4 and Cdc37, as well as an ~83 kDa protein. This was subsequently identified by mass spectrometry (MS) as the *Spodoptera frugiperda* Hsp90 homolog, which is >70% sequence identical to human Hsp90α. Subsequent purification yielded distinct fractions containing *H*sp90, *C*dc37, and Cd*k*4 (H-C-K) (Figure 1A) or *C*dc37 and Cd*k*4 (C-K) (Figure 2A), which eluted as single peaks in an analytical gel-filtration column, indicating that they are homogeneous ternary and binary complexes, respectively (Figures 1C and 2B).

Previous studies have shown that in the absence of a client kinase, Cdc37 and Hsp90 interact in vitro as dimers to form a $(Cdc37)_2$-$(Hsp90)_2$ complex (Roe et al., 2004; Roiniotis et al., 2005; Zhang et al., 2004). To determine the stoichiometries of the in vivo-assembled H-C-K and C-K complexes, the complexes were injected, using nanoelectrospray ionization, into a modified tandem time-of-flight (TOF) mass spectrometer (Waters Q-Tof2) that allows analysis of assembled protein complexes by minimizing the energy of molecular collisions and consequent dissociation of components (Sobott et al., 2002). M/z spectra for the H-C-K complex identified the presence of an $(Hsp90)_2$-Cdc37-Cdk4 complex, in addition to some uncomplexed protein generated by collisions in the spectrometer, but no larger species (Figures 1D and 1E). This stoichiometry is consistent with densitometry of the Coomassie-stained complex, which showed a 1:1 ratio of Cdc37 to Cdk4. The unusually heavy staining of Hsp90 is also consistent with our densitometry, which revealed Hsp90 to bind Coomassie in a nonlinear fashion when calibrated against Cdc37 and Cdk4 (Figure 1B). M/z spectra for the C-K fraction showed the presence of a $(Cdc37)_2$-Cdk4 complex, in addition to some uncomplexed protein generated by collisions in the spectrometer, but no larger assemblies (Figures 2C and 2D). As the 2:1:1 stoichiometry of the H-C-K complex was unexpected and in contradiction of our previous predictions (Roe et al., 2004), we sought to determine whether this was unique to complexes with Cdk4, or whether it represents the normal stoichiometry for stable Hsp90-Cdc37-kinase complexes. We therefore coexpressed the His_6-tagged kinase domain of B-Raf with Cdc37 in *Sf9* cells (Wan et al., 2004) and purified a B-Raf H-C-K complex in a similar fashion. As with the Cdk4 complex, modified QTOF MS of the B-Raf H-C-K complex identified an $(Hsp90)_2$-Cdc37-B-Raf complex as the largest species (see Figure S1 in the Supplemental Data available with this article online).

EM and 3D Reconstruction of an $(Hsp90)_2$-Cdc37-Cdk4 Complex

The small asymmetric H-C-K complex particles (~245 kDa) were visualized in the electron microscope at 42,000× magnification, stained with 2% uranyl acetate (Figure 3A). A total of 4231 individual particles were picked and aligned and grouped into classes by using multivariate statistical analysis and hierarchical ascendant classification (see Experimental Procedures). Stable representative classes were used to generate a 3D volume by angular reconstitution, which was iteratively refined to give the final model. Reprojections of the final model correspond well to the raw data (Figure 3B) and to the original classes from before the angular reconstitution, unbiased by the refinement process (Figure S2A). Particles showed a good angular distribution with no significant problems of preferred orientation (Figure S2B). The resolution of the structure, estimated from the Fourier shell correlation (FSC) coefficient of 0.5, is ~19 Å (Figure S2C).

The reconstructed H-C-K complex has an elongated structure that is ~140–150 Å long and ~85–95 Å in diameter, resembling a candle flame: pointed at one end and rounded at the other (Figure 4A). Two columns of density twist around the long axis, connecting the

Figure 1. Purification and Composition of the Hsp90-Cdc37-Cdk4 Ternary Complex

(A) 10% SDS-PAGE of purified H-C-K complex.

(B) Integrated optical density (IOD) for components of the H-C-K complex for four successive 2-fold dilutions in a Coomassie-stained 10% SDS-PAGE. The IOD was normalized by calculated molecular weight of each component and further normalized against the smallest component, Cdk4. The ratio of Cdc37 to Cdk4 remains 1:1 over successive dilutions, in agreement with results from MS (see Figure 1D). The Coomassie binding of Hsp90 is nonlinear, possibly as a consequence of the protein's very acidic nature.

(C) The final purification step is analytical gel filtration, and the chromatogram shows that the proteins run as a single species.

(D and E) The Nano-ESI TOF MS spectrum of the complex shows that the highest molecular weight species observed in the gas phase is a complex comprising a dimer of Hsp90, a monomer of Cdc37, and a monomer of Cdk4. Masses calculated from the sequences are as follows: Hsp90, 82,573 Da; Cdc37, 44,468 Da; Cdk4, 35,712 Da.

A

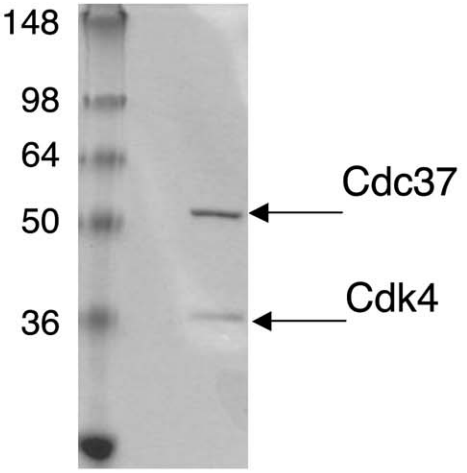

B

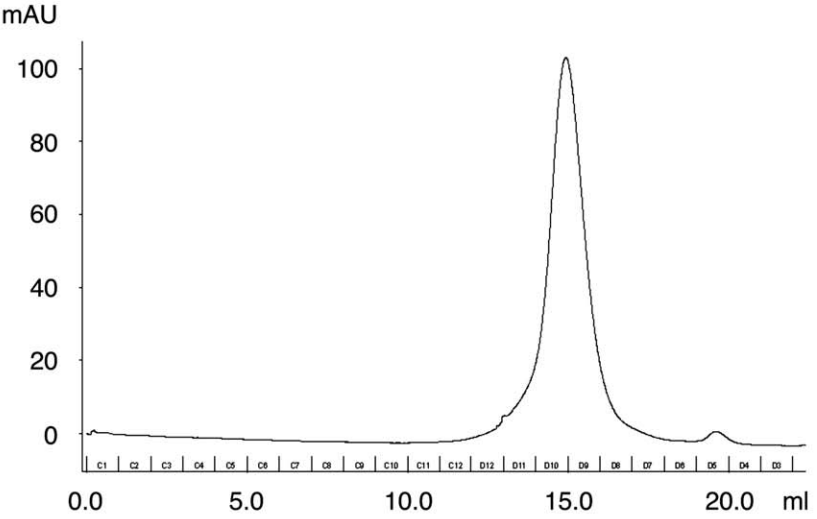

C

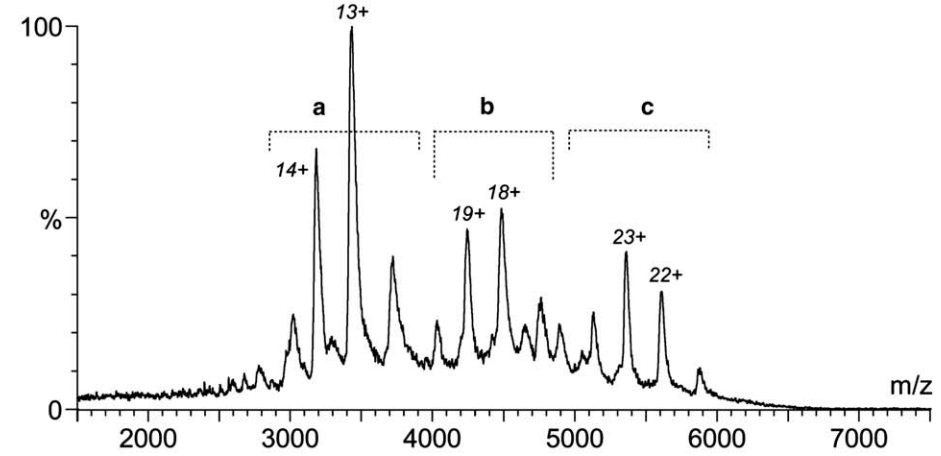

D

Peak series	Measured mass	Species
A	44 574 ±53 Da	Cdc37
B	80 679 ±43 Da	Cdc37 - Cdk4
C	123 384 ±63 Da	$(Cdc37)_2$ - Cdk4

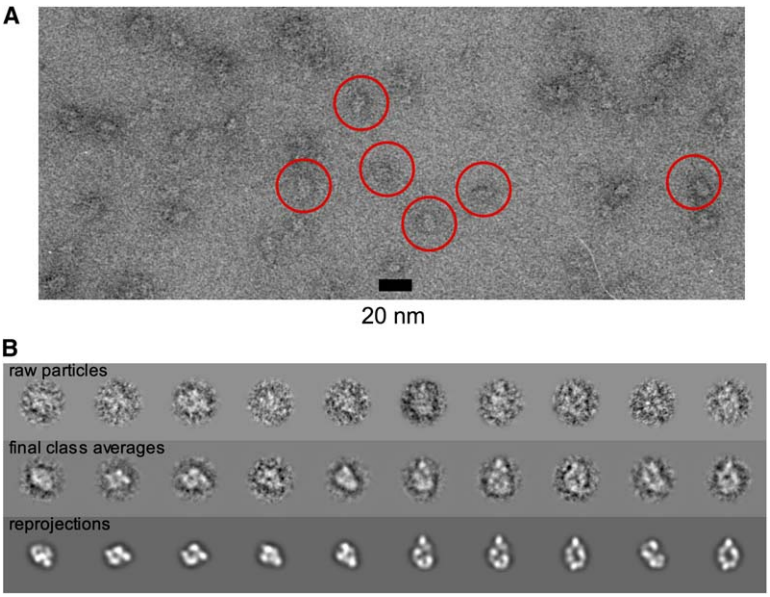

Figure 3. Negative-Stain EM of Hsp90-Cdc37-Cdk4 Complex

(A) A typical micrograph of 2% uranyl acetate-stained H-C-K showing views of the complex. Only particles that were well separated from the others and well stained were picked for analysis. Examples are highlighted in red.

(B) Reprojections from the model show features that are recognizable in typical raw particles. Some masked, centered raw particles retrospectively aligned to class averages generated by classification after the final alignment by projection matching. The corresponding reprojections of the model are shown below the class averages.

base to the narrower tip (Figure 4B). A stain-filled cavity evident in class sums corresponds to a channel of oval cross-section running through the 3D structure, perpendicular to the long axis. Views from opposite sides have many similarities, and there is overall a roughly 2-fold symmetry to the structure around the long axis. However, consistent with the 2:1:1 composition of the complex, this symmetry is approximate and is clearly broken by asymmetric distribution of density at the base and by a tilt to one side of the tip of the candle flame.

Fitting of Protein Chains

Comparison of the 3D reconstruction with the crystal structure of an Hsp90 dimer (Ali et al., 2006) shows many points of similarity, validating our angular reconstitution for this asymmetric complex (Figure 4C). Both crystal and EM structures have very similar overall shapes and dimensions, with a pointed and a rounded end; both structures have a narrow channel running through them, and both structures twist around the long axis (Figures 5A and 5B). The handedness of this latter feature allows the hand of the EM reconstruction to be fixed (Figure 5C). It is immediately evident from comparison with the crystal structure that the narrow tip of the EM volume corresponds to the constitutively dimerized C-terminal domains of Hsp90. The two partially symmetric longitudinal columns of density therefore correspond to the two Hsp90 monomers, with the N-terminal domains contributing to the rounded base of the reconstruction.

The columns of density connecting the tip and base are very similar in overall shape to monomers of Hsp90 from the crystal structure, and features corresponding to the three main segments of the Hsp90 crystal structure are readily discernible (Figures 5A and 5B). The individual monomers from the dimeric Hsp90 crystal structure could be readily docked into the density manually, maintaining the C-terminal dimerization interface. Small changes in domain orientation, achieved by hinging at the loop regions linking the domains, allow an excellent fit of the monomers to the reconstruction (Figure 6A). These segments of polypeptide are known to display considerable flexibility (see Discussion).

The N-terminal dimerization found in the crystal structure is not seen in the complex. Instead, the N-terminal domain of one monomer is hinged backward, away from its counterpart in the other monomer, such that its relative orientation with respect to the middle domain is opened like a jaw. For the second monomer, the largest change in domain orientation is between the C-terminal and middle domains, whereas orientation of the N-terminal domain relative to the middle domain is similar to that found in the crystal structure.

As well as the two Hsp90 molecules, the density of the EM reconstruction must account for the single Cdc37 and Cdk4 molecules present in the complex. The globular domain in the C-terminal half of Cdc37 has previously been shown to interact with the N-domain of Hsp90, binding to the lid and open mouth of the nucleotide binding pocket and preventing its interaction with the middle segment of the chaperone (Roe et al., 2004). The Hsp90 N-terminal domain from the crystal structure of the Hsp90-Cdc37 complex can be superposed onto the N-terminal domain of the "open" Hsp90 monomer (Figure 6A) in the EM reconstruction. This positions the Cdc37 C-terminal globular domain neatly into unoccupied density between the densities assigned to the two N-terminal domains of Hsp90.

The remaining unoccupied globular density is a bilobal segment bridging the base of the structure to halfway up one of the longitudinal columns. The lobes are of

Figure 2. Purification and Composition of the Cdc37-Cdk4 Binary Complex

(A) 10% SDS-PAGE of purified C-K complex.

(B) The final purification step is analytical gel filtration, and the chromatogram shows that the proteins run as a single species.

(C and D) The Nano-ESI TOF MS spectrum of the complex shows that the highest molecular weight species observed in the gas phase is a complex comprising a dimer of Cdc37 and a monomer of Cdk4. Masses calculated from the sequences are as follows: Cdc37, 44,468 Da; Cdk4, 35,712 Da.

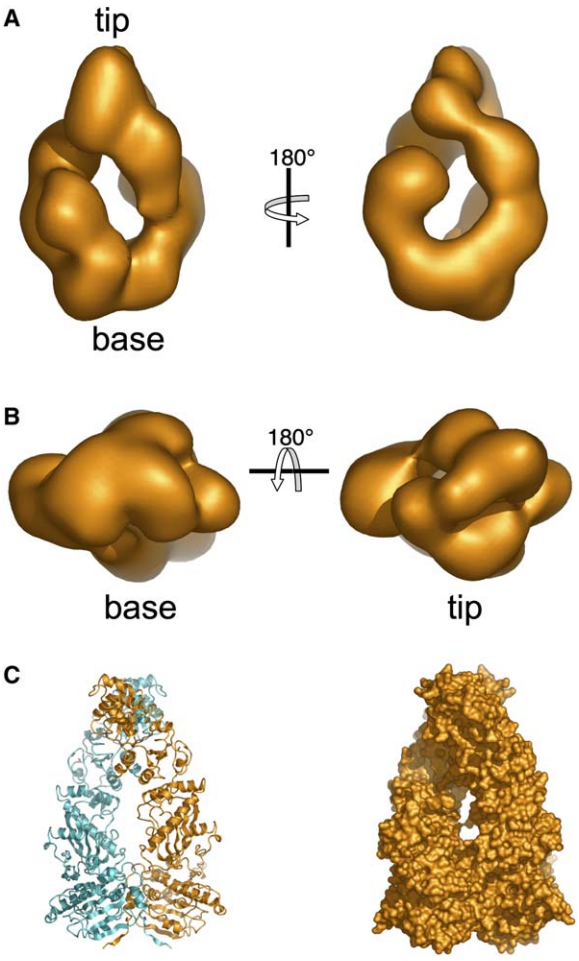

Figure 4. 3D Reconstruction of Hsp90-Cdc37-Cdk4 Complex

3D reconstruction of the H-C-K complex from negative-stain EM. (A) Side views (related by 180° rotation around the vertical)—the oval channel running through the center of the complex is immediately apparent, as are the two twisting columns of density connecting the base to the tip. (B) End views showing the tip (right) and base (left). (C) Secondary-structure cartoon (left) and molecular surface (right) of the Hsp90 dimer crystal structure (Ali et al., 2006). Models were generated using MacPyMOL (http://www.pymol.org).

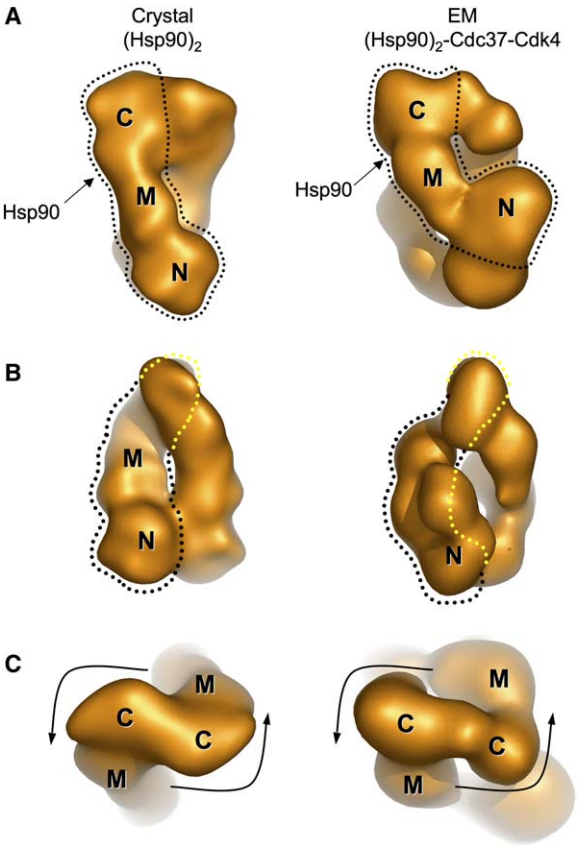

Figure 5. Architecture of the Hsp90-Cdc37-Cdk4 Complex

(A and B) Different views of the EM reconstruction, rotated around the vertical axis, and corresponding views of the crystal structure, filtered to 20 Å. Equivalent monomers in the crystal structure and the EM reconstruction are outlined in black for each view. By comparison of the two, domains of Hsp90 can be identified. Where one domain is hidden behind another, the outline is colored yellow. There are some interdomain movements on complexation with Cdc37 and Cdk4.

(C) The absolute hand of the EM reconstruction can be assigned by matching the twist of the two structures. The C-terminal domain is easily recognized, and therefore the polarity of Hsp90 within the model can be determined.

unequal size; the lower lobe, associated with the base of the reconstruction, is smaller than the upper lobe contacting the middle of one longitudinal column. The sizes of these lobes are consistent with the N-terminal and C-terminal lobes, respectively, of a cyclin-dependent kinase catalytic domain (Figure 6A).

There is no distinct globular density that can be assigned to the N-terminal segment of Cdc37, whose structure is currently unknown. However, there is continuous extra density around the N-terminal domain of the second Hsp90 (Figure 6B). The orientation of the docked C-terminal Cdc37 globular domain directs the helix connecting to the N-terminal domain into this extra density. As we find that Cdc37-pSer13 in the complex is highly resistant to dephosphorylation (data not shown), the N terminus of Cdc37 appears to be considerably buried in the complex, and it is likely that it is subsumed in the density at the base of the reconstruction, closely associated with the Hsp90 N-terminal domains and the kinase and probably in contact with both. No density for the C-terminal tail of Cdc37 is visible in the reconstruction; however, on the basis of the orientation of the docked Cdc37 globular domain, this helical segment would be directed out of the complex into solvent and would be unlikely to be well ordered. Indeed, in the crystal structure of Cdc37 bound to the N terminus of Hsp90, the C-terminal tail displayed high temperature factors and was only visible as a result of a fortuitous crystal contact (Roe et al., 2004). Consistent with the lack of any direct involvement of this C-terminal tail in the complex, the corresponding region has been shown to be substantially dispensable for full biological function in yeast (Lee et al., 2002).

Discussion

Conformational Flexibility of Hsp90

Comparison of Hsp90 crystal structures illustrates the molecule's considerable flexibility. For example, alignment of the middle domains of yeast Hsp90 (Ali et al., 2006) with their equivalent in the *E. coli* homolog HtpG

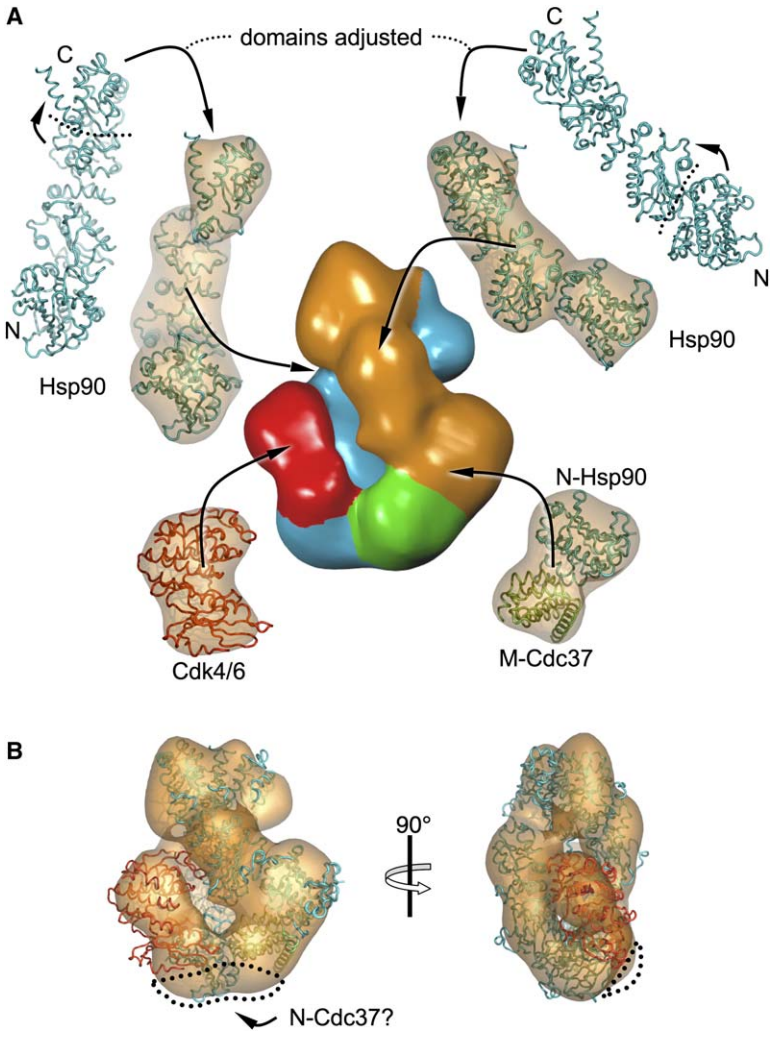

Figure 6. Modeling Cdc37 and Cdk4

(A) The relative orientations of domains of the crystal structure of Hsp90 are adjusted by small rotations in the hinge regions and fitted into the EM reconstruction. The location of M-Cdc37 is determined by a least-squares fit of the N-terminal domain of the open monomer with N-Hsp90 from the crystal structure of the complex with Cdc37. Cdk6 is used as a model for Cdk4. The larger C-terminal lobe of the kinase fills the larger lobe of the reconstruction and consequently is intimately associated with the middle domain of one Hsp90 monomer. The N-terminal lobe is smaller and fills the remaining density, associating with either the N-terminal domain of Hsp90 or Cdc37, or both. Atomic models are shown superimposed on their molecular volumes filtered to 20 Å resolution. The EM reconstruction is colored according to protein chain: Hsp90 open monomer, orange; Hsp90 closed monomer, blue; Cdc37, green; Cdk4, red.

(B) Orthogonal views of the pseudoatomic model of the $(Hsp90)_2$-Cdc37-Cdk4 complex docked into the EM reconstruction. Some unassigned density in the vicinity of the Hsp90 N termini (dotted outline) could accommodate the N-terminal domain of Cdc37, whose structure is not known but is predicted to contain a segment of coiled coil and could bridge to the N-terminal domain of the closed Hsp90 monomer and/or the bound kinase.

(Huai et al., 2005) reveals a huge translation and rotation of the N domain in each structure with respect to the other, such that the β sheets therein are now at right angles. This degree of flexibility within the confines of a crystal lattice reflects a much greater conformational variability revealed by analysis of the Hsp90 dimer in solution (Zhang et al., 2004). Indeed, difficulty in obtaining crystals of the full-length protein that diffract to high resolution can be attributed to this conformational variability. Success was ultimately dependent on trapping Hsp90 in a defined functional and conformational state, in complex with nucleotide and the cochaperone p23/Sba1 (Ali et al., 2006).

Biochemical and structural data to date support an ATP-driven molecular clamp mechanism (Prodromou et al., 2000; Siligardi et al., 2004), and large conformational changes of the type described above are a prerequisite for this. The Hsp90 dimer, constitutively dimerized via its C-terminal domains, cycles between a state in which the N-terminal domains are in an open, ATP-free conformation, either held apart in a rigid manner by a dimer of the cochaperone Cdc37 (Roe et al., 2004) or simply unconstrained, and a closed or tense state in which ATP is bound and a lid is closed over the ATP binding site to expose a second, transient dimerization interface between the two N-terminal domains (Ali et al., 2006; Prodromou et al., 2000).

The flexibility required for such large structural changes can been attributed to two linker regions that join the N-terminal to middle, and middle to C-terminal domains. The flexibility of these linkers is evident from their susceptibility to proteolysis, and the stability of the domains they connect when expressed in isolation. In our model, the crystal structure of full-length Hsp90 fits into the EM reconstruction with relatively small adjustments of these linker regions. The dynamic nature of Hsp90's structure is therefore important not only for the hydrolysis of ATP (Prodromou et al., 2000) and cochaperone binding (Meyer et al., 2004; Roe et al., 2004) but also for enabling Hsp90 to adopt conformations, such as we see in the current reconstruction, which allow client protein binding.

Protein Kinase and Cdc37 Interactions

A significant number of protein kinases form complexes with Hsp90 and Cdc37 as a prerequisite to their activation (reviewed in Pearl [2005]), but the stoichiometry of these complexes has not previously been determined. For Cdk4 and for B-Raf, we have now observed a stable complex containing an Hsp90 dimer bound to single

molecules of Cdc37 and the kinase, affinity purified via the tagged kinase. Whether this stoichiometry is common to all kinase clients of Hsp90 is not known, but that it occurs with two such distantly related kinases suggests that this is likely to be the case. By contrast, the Cdc37-Cdk4 complex devoid of Hsp90 contains a single kinase bound to a dimer of Cdc37. We and others have previously shown formation of an Hsp90-Cdc37 complex in the absence of any kinase, consisting of dimers of each (Roe et al., 2004; Roiniotis et al., 2005; Zhang et al., 2004). Cdc37 is a dimer in isolation, but its dissociation constant is low micromolar (Siligardi et al., 2002), suggesting that it can exist happily in dimer or monomer form. Taken together, these data point to an ordered process of kinase client loading in which a kinase-$(Cdc37)_2$ complex initially binds to an Hsp90 dimer via a symmetrical $(Cdc37)_2$-$(Hsp90)_2$ dimer-dimer interaction, as previously suggested (Roe et al., 2004), that simultaneously arrests the ATPase cycle of Hsp90 (Siligardi et al., 2002). Subsequent conformational rearrangement of that initial complex could then release a Cdc37 molecule to give the stable asymmetrical $(Hsp90)_2$-Cdc37-kinase complexes reported here (Figure S3). While this idea is fully consistent with the data, further work will be required to substantiate it.

The channel between the Hsp90 protomers in the complex clearly contradicts previous models (Roe et al., 2004) in which a client is bound between the two Hsp90 molecules in an analogy to "barrel" chaperonins such as GroEL or CCT (Saibil, 2000). Instead, the client is bound to the outer edge of one Hsp90 molecule, bridging its N-terminal and middle segments. The density attributed to Cdk4 is distinctly bilobal, suggesting that the two lobes of the kinase are in an extended conformation compared with the mature protein. This could have consequences for the ability of the kinase to bind nucleotide, since motifs from both lobes contribute to the ATP binding site. Whether Cdk4 is competent to bind ATP, cyclins, or CDK inhibitory proteins when part of the Hsp90-Cdc37 complex is now the focus of further work in our laboratory.

The larger lobe of the kinase clearly interacts with the middle segment of one Hsp90 monomer, while the other lobe is in a position to interact with the associated Hsp90 N-terminal domain and/or N-terminal part of the Cdc37 molecule anchored on the other Hsp90 N-terminal domain; these possibilities cannot be distinguished in the present structure and may occur simultaneously. This complex mode of interaction is consistent with studies analyzing sites of interaction between Hsp90, Cdc37, and a range of client protein kinases including ErbB2 (Xu et al., 2005), HRI (Scroggins et al., 2003), Lck (Prince and Matts, 2004), as well as Cdk4 (Zhao et al., 2004), that implicate the N-terminal lobe of the kinase as essential for interactions with Hsp90 and Cdc37, while regions in the kinase C terminus are involved in Hsp90 binding only. Our interpretation of the bilobal segments, based on their size (see Results), is fully consistent with these analyses. In addition, the larger lobe of the kinase density comes close to a hydrophobic patch centered on Trp300 in the middle segment of Hsp90 and shown by mutagenesis to be involved in client protein binding (Meyer et al., 2003) (Figure 7). Part of this patch is contributed by residues 328–338, which form an amphipathic loop

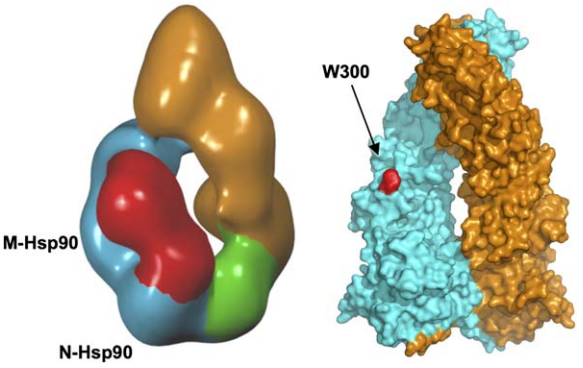

Figure 7. Client Protein Interactions

Comparison of the ~19 Å single-particle EM reconstruction (left) of an $(Hsp90)_2$-Cdc37-Cdk4 complex with the ATP bound Hsp90 crystal structure (right). The bilobal kinase client (red) appears to interact with the N domain of one Hsp90 protomer and a region on the middle segment close to Trp300 (red on left), which is implicated in client protein binding. Changes in relative position of these Hsp90 domains coupled to the ATPase cycle would be transmitted to the bound client protein.

projecting from the body of the middle segment. The considerable flexibility of this loop would give a degree of tolerance allowing interaction with a range of client proteins.

The bivalent interaction of the Cdk4, with one lobe binding to the middle segment of Hsp90 and the other to the N-terminal domain and/or Cdc37, provides a clear mechanism for coupling ATP-dependent changes in the relative conformation of the N-terminal and middle segments of Hsp90 (Chadli et al., 2000; Prodromou et al., 2000) to changes in the orientation of the N and C lobes of the bound kinase. As the relative positioning of these lobes and the segment of protein that links them is well known to play a significant role in regulating the activity of many protein kinases (Johnson et al., 1996), association with Hsp90 might be required to facilitate the switch from an inactive to an active conformation in those kinases where there is a high activation barrier to that conformational change.

The N-terminal domain of Cdc37 has consistently been shown to be necessary for kinase binding (Grammatikakis et al., 1999; Shao et al., 2001), while its C terminus is responsible for interaction with Hsp90 (Roe et al., 2004; Shao et al., 2001; Zhang et al., 2004). Nonetheless, the extreme N-terminal part of Cdc37 also plays a role in Hsp90 interactions in the context of a client protein complex. Thus, while mutation of residues 2–4 of Cdc37 compromises binding of a client kinase but does not affect Hsp90 binding (Scroggins et al., 2003), mutation of Trp7 results in reduced binding for both client and Hsp90. Phosphorylation of Ser13 in Cdc37 has been shown to be essential for formation of productive Hsp90-Cdc37-client complexes, but mutation of this residue has no apparent effect on direct Hsp90-Cdc37 interaction (Miyata and Nishida, 2004; Shao et al., 2003b). We find this phosphorylation to be present in the purified baculovirus-expressed Cdc37 and in $(Hsp90)_2$-Cdc37-Cdk4 complexes. pSer13 in free Cdc37 is rapidly dephosphorylated by phosphatase treatment; however, in marked contrast, pSer13 in the ternary $(Hsp90)_2$-Cdc37-Cdk4 complex was resistant to dephosphorylation,

consistent with its burial in the complex (data not shown). Taken together, these data suggest that the extreme N-terminal segment of Cdc37 incorporating pSer13 cements the interaction between Hsp90 and the kinase client, possibly becoming bound between them in the ternary complex.

In our model, the N-terminal segment of Cdc37 would stretch across the base of the complex toward the bound Cdk4 and the other Hsp90 N-terminal domain, allowing residues at its N terminus to interact with both as suggested by the mutational and accessibility data. This is also consistent with the additional observation that the residues in Cdc37 that connect its N-terminal and C-terminal domains regulate both Hsp90 and kinase binding, since it is this subdomain of Cdc37 that would bridge between the N-terminal domains of the two Hsp90 monomers (Shao et al., 2003b).

A recent study examining the client binding site on Cdc37 isolated a hydrophobic 20-residue peptide corresponding to residues 181–200 of Cdc37 that could apparently coprecipitate Raf-1 kinase domain from COS-7 cells (Terasawa and Minami, 2005). The significance of this observation is uncertain, as these residues are substantially buried in the globular domain of Cdc37 that binds the N-terminal domain of Hsp90 (Roe et al., 2004). Furthermore, these results directly conflict with earlier studies in COS-1 and *Sf9* cells, which showed that the Raf-1 kinase binding site on Cdc37 resides in the N-terminal half of the protein (residues 1–164) (Grammatikakis et al., 1999) and that truncation of Cdc37 beyond residue 164 results in loss of Hsp90 from the Cdc37-Raf-1 complex, consistent with our crystallographic data (Roe et al., 2004).

Conclusion

The EM reconstruction presented here provides a first experimental view of a client-loaded Hsp90 complex. The exact orientation of each domain within the complex, the nature of the interaction of the N-terminal domain of Cdc37 with Hsp90 and Cdk4, and the detailed interactions of residues at the protein-protein interfaces within the complex cannot be resolved at the resolution accessible with negative-stain EM. Nevertheless, within the context of these limitations, the composition and architecture of the Hsp90-Cdc37-kinase complex can be defined and our interpretation is consistent with a large body of crystallographic, biochemical, and genetic data published to date.

This complex was isolated in the presence of sodium molybdate, which has been widely used to stabilize complexes of steroid hormone receptors and other transcription factors with Hsp90 (Pratt and Toft, 1997) and which has the same effect here (see Experimental Procedures). Molybdate is believed to act as a mimetic of the ATP γ-phosphate, occupying Hsp90's ATP binding site in combination with ADP to inhibit the ATPase cycle and trap the complex with the client in a preactivated "early" state. The precise position in the chaperone cycle that our reconstruction represents is not known. However, the presence of one Cdc37 molecule suggests that it is also an early complex, trapped somewhere between initial complex formation, which involves a Cdc37 dimer (Siligardi et al., 2002; Zhang et al., 2004), and the catalytically competent ATP bound conformation (Ali et al., 2006), progression to which requires complete disengagement of Cdc37 from the Hsp90 N domains. In any event, this complex is only one of a number of modes of interaction that a client makes with Hsp90 and Cdc37 during the chaperone's ATPase cycle, and further work will be required to identify and isolate the other client bound intermediates that may occur.

Many key questions related to the detailed interactions involved remain to be answered. It is only those details that will lead to a full understanding of how Hsp90 and Cdc37 facilitate activation of client protein kinases, and to a determination of what features of the client proteins are responsible for their specific requirement for, and recruitment to, the Hsp90-Cdc37 chaperone system. Full activation of Cdk4, downstream of Hsp90 binding, requires phosphorylation of the activation loop, and complexation with cyclin D (Kato et al., 1994). Whether these steps take place in the context of Hsp90 is at present unknown, but the Hsp90-Cdc37-Cdk4 complex provides a robust system with which to address these questions.

Experimental Procedures

Expression and Purification of Proteins

A modified pFastBac DUAL (Invitrogen) expression vector was made by inserting an intergenic region, encoding a His_6 tag, between BamHI and EcoRI of multiple cloning site I (MCS I). This modification also encoded an NheI restriction site immediately 3′ to the His_6 tag. The *CDK4* gene was amplified by PCR. The primers used encoded a BamHI and NheI restriction site, and a PreScission cleavage site, all 5′ to the gene, and a HindIII restriction site 3′ to the gene. The BamHI-HindIII fragment was cloned into pET28a (Novagen). Subsequently, the NheI-NotI fragment was cloned into our modified MCS I of pFastBac DUAL. Cloning of human *Cdc37* has been described previously (Siligardi et al., 2002). A XhoI/KpnI PCR fragment of *Cdc37* was cloned into MCS II of the pFastBac DUAL vector.

Proteins were expressed in *Sf9* cells over 3 days. The cell pellet was lysed by homogenization in TBS-Mo buffer (25 mM Tris-HCl [pH 7.5], 150 mM NaCl, 10 mM KCl, 10 mM $MgCl_2$, and 20 mM Na_2MoO_4) with 25 mM NaF, 25 mM β-sodium glycerophosphate, and EDTA-free complete protease inhibitor tablets (Roche). *C*dc37 and C*dk4* coeluted with endogenous *Sf9 H*sp90 (H-C-K) from TALON resin (BD Biosciences). Gel filtration on a Superdex200 HR column (GE Healthcare) with TBS-Mo buffer; desalting into TBS-Mo without NaCl, followed by ion exchange using Q-Source resin (GE Healthcare); and analytical gel filtration on a Superose 6 HR10/30 (GE Healthcare) column with TBS-Mo buffer were used to purify the complex to homogeneity. The complex could also be isolated by using the same protocol in the absence of sodium molybdate; however, the yields were considerably reduced. Baculovirus-expressed Hsp90-Cdc37-B-Raf complex was purifed as described (Wan et al., 2004).

Nano-ESI TOF MS

Samples for MS analysis were buffer exchanged into 100 mM ammonium acetate (pH 7), using Micro Bio-Spin 6 columns (Bio-Rad). Nano-ESI capillaries were prepared in-house from borosilicate glass tubes of 1 mm outer and 0.5 mm inner diameter (Harvard Apparatus, Holliston, Massachusetts) using a Flaming/Brown P-97 micropipette puller (Sutter Instruments, Hercules, California) and were gold coated using a sputter coater (Quorum Technologies, Newhaven, United Kingdom). Capillary tips were cut under a stereomicroscope to give inner diameters of 1–5 μm, and typically 2 μl of solution was loaded for sampling. Mass spectra were recorded on a tandem mass spectrometer (Waters Q-Tof2, Manchester, United Kingdom) that was modified for high-mass operation (Sobott et al., 2002), and pressures and accelerating potentials were adjusted to preserve noncovalent interactions (Heck and Van Den Heuvel, 2004; Sobott and Robinson, 2002). Data were acquired and processed with MassLynx software (Waters, Manchester, United Kingdom).

Electron Microscopy

HCK complex at 10–15 μg/ml was stained on carbon-coated copper grids with 2% (w/v) uranyl acetate after glow discharging in the presence of pentyl-amine. Samples were imaged in an FEI Tecnai T12 electron microscope (FEI, Eindhoven, The Netherlands) operating at 120kV and were recorded in low-dose mode at a defocus of around 0.5 μm on Kodak SO163 film at 42,000× magnification. Micrographs were digitized on a Zeiss PhotoScan LD linear array scanner at 14 μm/pixel (3.33 Å/pixel at the specimen level).

Image Processing

Defocus and astigmatism were determined using CTFfind3 (Mindell and Grigorieff, 2003). Boxed particles from 35 micrographs were imported into IMAGIC (van Heel et al., 1996) for all further processing. A total of 4231 particles were centered using three rounds of translational alignment to the rotationally averaged total sum. Multivariate statistical analysis and hierarchical ascendant classification were used to generate reference classes to which all particles were aligned. This process was repeated iteratively. Well-defined classes representing distinct views of the complex were chosen for angular reconstitution to generate an initial model. Additional classes were incorporated into the model with increasing Euler angle precision in three rounds of anchor set refinement.

At this point, the reconstruction was 3D masked and refined by projection matching. For each iteration, the angle assignments were sorted by reprojection error (agreement between the average for each orientation and the corresponding reprojection) and visually checked to ensure that the classes were acceptable. A 3D map was then created from the acceptable classes.

The model was determined to be fully refined after eight rounds of projection matching, when the percentage of total particles changing class between successive rounds and the value of the FSC coefficient at 0.5 had converged. At this stage, there was no visible change in the reconstruction between rounds of refinement. The final reconstruction was generated using 190 out of a total of 412 class sums, containing 76.8% of the data, but a map with all 412 sums was not noticeably different.

Model Building

The anticlockwise twist of the crystal structure of full-length Hsp90 (Ali et al., 2006) was used to assign the hand of the EM map.

All crystal structures used for model building (Hsp90, PDB code 2CGE, 2CG9; Cdk6, PDB code 1J0W; N-Hsp90-C-Cdc37, PDB code 1US7) were filtered to 20 Å using the Situs program PDBlur (Wriggers et al., 1999) to allow a direct comparison with the EM reconstruction. All docking was carried out manually in MacPyMOL (www.pymol.org).

Supplemental Data

Supplemental Data include three figures and Supplemental References and can be found with this article online at http://www.molecule.org/cgi/content/full/23/5/697/DC1/.

Acknowledgments

We are very grateful to Paul Wan and Chris Marshall for the kind gifts of B-Raf-Hsp90-Cdc37 complex and Cdk4 cDNA, respectively; to Vivienne Thompson and Sara Kisakye-Nambozo for assistance with baculovirus expression; and to Elena Orlova for help with angular reconstitution. This work was supported by BBSRC (H.R.S.) and the Wellcome Trust (L.H.P.).

Received: March 21, 2006
Revised: May 13, 2006
Accepted: July 5, 2006
Published: August 31, 2006

References

Ali, M.M., Roe, S.M., Vaughan, C.K., Meyer, P., Panaretou, B., Piper, P.W., Prodromou, C., and Pearl, L.H. (2006). Crystal structure of an Hsp90-nucleotide-p23/Sba1 closed chaperone complex. Nature *440*, 1013–1017.

Basso, A.D., Solit, D.B., Chiosis, G., Giri, B., Tsichlis, P., and Rosen, N. (2002). Akt forms an intracellular complex with heat shock protein 90 (Hsp90) and Cdc37 and is destabilized by inhibitors of Hsp90 function. J. Biol. Chem. *277*, 39858–39866.

Bijlmakers, M.J., and Marsh, M. (2000). Hsp90 is essential for the synthesis and subsequent membrane association, but not the maintenance, of the Src-kinase p56(lck). Mol. Biol. Cell *11*, 1585–1595.

Boudeau, J., Deak, M., Lawlor, M.A., Morrice, N.A., and Alessi, D.R. (2003). Heat-shock protein 90 and Cdc37 interact with LKB1 and regulate its stability. Biochem. J. *370*, 849–857.

Brugge, J.S. (1986). Interaction of the Rous sarcoma virus protein pp60v-src with the cellular proteins pp50 and pp90. Curr. Top. Microbiol. Immunol. *123*, 1–22.

Chadli, A., Bouhouche, I., Sullivan, W., Stensgard, B., McMahon, N., Catelli, M.G., and Toft, D.O. (2000). Dimerization and N-terminal domain proximity underlie the function of the molecular chaperone heat shock protein 90. Proc. Natl. Acad. Sci. USA *97*, 12524–12529.

Chen, G., Cao, P., and Goeddel, D.V. (2002). TNF-induced recruitment and activation of the IKK complex require Cdc37 and Hsp90. Mol. Cell *9*, 401–410.

Dai, K., Kobayashi, R., and Beach, D. (1996). Physical interaction of mammalian CDC37 with CDK4. J. Biol. Chem. *271*, 22030–22034.

Fontana, J., Fulton, D., Chen, Y., Fairchild, T.A., McCabe, T.J., Fujita, N., Tsuruo, T., and Sessa, W.C. (2002). Domain mapping studies reveal that the M domain of hsp90 serves as a molecular scaffold to regulate Akt-dependent phosphorylation of endothelial nitric oxide synthase and NO release. Circ. Res. *90*, 866–873.

Fujita, N., Sato, S., Ishida, A., and Tsuruo, T. (2002). Involvement of Hsp90 in signaling and stability of 3-phosphoinositide-dependent kinase-1. J. Biol. Chem. *277*, 10346–10353.

Grammatikakis, N., Lin, J.-H., Grammatikakis, A., Tsichlis, P.N., and Cochran, B.H. (1999). p50cdc37 acting in concert with Hsp90 is required for Raf-1 function. Mol. Cell. Biol. *19*, 1661–1672.

Heck, A.J., and Van Den Heuvel, R.H. (2004). Investigation of intact protein complexes by mass spectrometry. Mass Spectrom. Rev. *23*, 368–389.

Huai, Q., Wang, H., Liu, Y., Kim, H.Y., Toft, D., and Ke, H. (2005). Structures of the N-terminal and middle domains of E. coli Hsp90 and conformation changes upon ADP binding. Structure *13*, 579–590.

Johnson, L.N., Noble, M.E.M., and Owen, D.J. (1996). Active and inactive protein kinases: structural basis for regulation. Cell *85*, 149–158.

Kato, J.Y., Matsuoka, M., Strom, D.K., and Sherr, C.J. (1994). Regulation of cyclin D-dependent kinase 4 (cdk4) by cdk4-activating kinase. Mol. Cell. Biol. *14*, 2713–2721.

Lamphere, L., Fiore, F., Xu, X., Brizuela, L., Keezer, S., Sardet, C., Draetta, G.F., and Gyuris, J. (1997). Interaction between Cdc37 and Cdk4 in human cells. Oncogene *14*, 1999–2004.

Lange, B.M., Rebollo, E., Herold, A., and Gonzalez, C. (2002). Cdc37 is essential for chromosome segregation and cytokinesis in higher eukaryotes. EMBO J. *21*, 5364–5374.

Lee, P., Rao, J., Fliss, A., Yang, E., Garrett, S., and Caplan, A.J. (2002). The Cdc37 protein kinase-binding domain is sufficient for protein kinase activity and cell viability. J. Cell Biol. *159*, 1051–1059.

Lewis, J., Devin, A., Miller, A., Lin, Y., Rodriguez, Y., Neckers, L., and Liu, Z.G. (2000). Disruption of hsp90 function results in degradation of the death domain kinase, receptor-interacting protein (RIP), and blockage of tumor necrosis factor-induced nuclear factor-kappaB activation. J. Biol. Chem. *275*, 10519–10526.

Mahony, D., Parry, D.A., and Lees, E. (1998). Active cdk6 complexes are predominantly nuclear and represent only a minority of the cdk6 in T cells. Oncogene *16*, 603–611.

Meyer, P., Prodromou, C., Hu, B., Vaughan, C., Roe, S.M., Panaretou, B., Piper, P.W., and Pearl, L.H. (2003). Structural and functional analysis of the middle segment of Hsp90: implications for ATP hydrolysis and client-protein and co-chaperone interactions. Mol. Cell *11*, 647–658.

Meyer, P., Prodromou, C., Liao, C., Hu, B., Mark Roe, S., Vaughan, C.K., Vlasic, I., Panaretou, B., Piper, P.W., and Pearl, L.H. (2004). Structural basis for recruitment of the ATPase activator Aha1 to the Hsp90 chaperone machinery. EMBO J. *23*, 511–519.

Mindell, J.A., and Grigorieff, N. (2003). Accurate determination of local defocus and specimen tilt in electron microscopy. J. Struct. Biol. *142*, 334–347.

Miyata, Y., and Nishida, E. (2004). CK2 controls multiple protein kinases by phosphorylating a kinase-targeting molecular chaperone, Cdc37. Mol. Cell. Biol. *24*, 4065–4074.

O'Keeffe, B., Fong, Y., Chen, D., Zhou, S., and Zhou, Q. (2000). Requirement for a kinase-specific chaperone pathway in the production of a Cdk9/cyclin T1 heterodimer responsible for P-TEFb-mediated tat stimulation of HIV-1 transcription. J. Biol. Chem. *275*, 279–287.

Pearl, L.H. (2005). Hsp90 and Cdc37—a chaperone cancer conspiracy. Curr. Opin. Genet. Dev. *15*, 55–61.

Pratt, W.B., and Toft, D.O. (1997). Steroid receptor interactions with heat shock protein and immunophilin chaperones. Endocr. Rev. *18*, 306–360.

Prince, T., and Matts, R.L. (2004). Definition of protein kinase sequence motifs that trigger high affinity binding of Hsp90 and Cdc37. J. Biol. Chem. *279*, 39975–39981.

Prodromou, C., Roe, S.M., O'Brien, R., Ladbury, J.E., Piper, P.W., and Pearl, L.H. (1997). Identification and structural characterization of the ATP/ADP-binding site in the Hsp90 molecular chaperone. Cell *90*, 65–75.

Prodromou, C., Panaretou, B., Chohan, S., Siligardi, G., O'Brien, R., Ladbury, J.E., Roe, S.M., Piper, P.W., and Pearl, L.H. (2000). The ATPase cycle of Hsp90 drives a molecular 'clamp' via transient dimerization of the N-terminal domains. EMBO J. *19*, 4383–4392.

Roe, S.M., Prodromou, C., O'Brien, R., Ladbury, J.E., Piper, P.W., and Pearl, L.H. (1999). The structural basis for inhibition of the Hsp90 molecular chaperone by the antitumor antibiotics radicicol and geldanamycin. J. Med. Chem. *42*, 260–266.

Roe, S.M., Ali, M.M., Meyer, P., Vaughan, C.K., Panaretou, B., Piper, P.W., Prodromou, C., and Pearl, L.H. (2004). The mechanism of Hsp90 regulation by the protein kinase-specific cochaperone p50(cdc37). Cell *116*, 87–98.

Roiniotis, J., Masendycz, P., Ho, S., and Scholz, G.M. (2005). Domain-mediated dimerization of the Hsp90 cochaperones Harc and Cdc37. Biochemistry *44*, 6662–6669.

Saibil, H. (2000). Molecular chaperones: containers and surfaces for folding, stabilising or unfolding proteins. Curr. Opin. Struct. Biol. *10*, 251–258.

Sato, S., Fujita, N., and Tsuruo, T. (2000). Modulation of akt kinase activity by binding to hsp90. Proc. Natl. Acad. Sci. USA *97*, 10832–10837.

Schulte, T.W., Blagosklonny, M.V., Ingui, C., and Neckers, L. (1995). Disruption of the Raf-1-Hsp90 molecular complex results in destabilization of Raf-1 and loss of Raf-1-Ras association. J. Biol. Chem. *270*, 24585–24588.

Scroggins, B.T., Prince, T., Shao, J., Uma, S., Huang, W., Guo, Y., Yun, B.G., Hedman, K., Matts, R.L., and Hartson, S.D. (2003). High affinity binding of Hsp90 is triggered by multiple discrete segments of its kinase clients. Biochemistry *42*, 12550–12561.

Shao, J., Grammatikakis, N., Scroggins, B.T., Uma, S., Huang, W.J., Chen, J.J., Hartson, S.D., and Matts, R.L. (2001). Hsp90 regulates p50(cdc27) function during the biogenesis of the active conformation of the heme-regulated eIF2 alpha kinase. J. Biol. Chem. *276*, 206–214.

Shao, J., Irwin, A., Hartson, S.D., and Matts, R.L. (2003a). Functional dissection of cdc37: characterization of domain structure and amino acid residues critical for protein kinase binding. Biochemistry *42*, 12577–12588.

Shao, J., Prince, T., Hartson, S.D., and Matts, R.L. (2003b). Phosphorylation of serine 13 is required for the proper function of the Hsp90 co-chaperone, Cdc37. J. Biol. Chem. *278*, 38117–38120.

Siligardi, G., Panaretou, B., Meyer, P., Singh, S., Woolfson, D.N., Piper, P.W., Pearl, L.H., and Prodromou, C. (2002). Regulation of Hsp90 ATPase activity by the co-chaperone Cdc37p/p50^{cdc37}. J. Biol. Chem. *277*, 20151–20159.

Siligardi, G., Hu, B., Panaretou, B., Piper, P.W., Pearl, L.H., and Prodromou, C. (2004). Co-chaperone regulation of conformational switching in the Hsp90 ATPase cycle. J. Biol. Chem. *279*, 51989–51998.

Silverstein, A.M., Grammatikakis, N., Cochran, B.H., Chinkers, M., and Pratt, W.B. (1998). P50(cdc37) binds directly to the catalytic domain of Raf as well as to a site on hsp90 that is topologically adjacent to the tetratricopeptide repeat binding site. J. Biol. Chem. *273*, 20090–20095.

Sobott, F., and Robinson, C.V. (2002). Protein complexes gain momentum. Curr. Opin. Struct. Biol. *12*, 729–734.

Sobott, F., Hernandez, H., McCammon, M.G., Tito, M.A., and Robinson, C.V. (2002). A tandem mass spectrometer for improved transmission and analysis of large macromolecular assemblies. Anal. Chem. *74*, 1402–1407.

Stancato, L.F., Chow, Y.-H., Hutchinson, K.A., Perdew, G.H., Jove, R., and Pratt, W.B. (1993). Raf exists in a native heterocomplex with Hsp90 and p50 that can be reconstituted in a cell-free system. J. Biol. Chem. *268*, 21711–21716.

Stebbins, C.E., Russo, A.A., Schneider, C., Rosen, N., Hartl, F.U., and Pavletich, N.P. (1997). Crystal structure of an Hsp90-geldanamycin complex: targeting of a protein chaperone by an antitumor agent. Cell *89*, 239–250.

Stepanova, L., Leng, X.H., Parker, S.B., and Harper, J.W. (1996). Mammalian p50(Cdc37) is a protein kinase-targeting subunit of Hsp90 that binds and stabilizes Cdk4. Genes Dev. *10*, 1491–1502.

Stepanova, L., Finegold, M., DeMayo, F., Schmidt, E.V., and Harper, J.W. (2000a). The oncoprotein kinase chaperone CDC37 functions as an oncogene in mice and collaborates with both c-myc and cyclin D1 in transformation of multiple tissues. Mol. Cell. Biol. *20*, 4462–4473.

Stepanova, L., Yang, G., DeMayo, F., Wheeler, T.M., Finegold, M., Thompson, T.C., and Harper, J.W. (2000b). Induction of human Cdc37 in prostate cancer correlates with the ability of targeted Cdc37 expression to promote prostatic hyperplasia. Oncogene *19*, 2186–2193.

Terasawa, K., and Minami, Y. (2005). A client-binding site of Cdc37. FEBS J. *272*, 4684–4690.

van Heel, M., Harauz, G., Orlova, E.V., Schmidt, R., and Schatz, M. (1996). A new generation of the IMAGIC image processing system. J. Struct. Biol. *116*, 17–24.

Wan, P.T., Garnett, M.J., Roe, S.M., Lee, S., Niculescu-Duvaz, D., Good, V.M., Jones, C.M., Marshall, C.J., Springer, C.J., Barford, D., and Marais, R. (2004). Mechanism of activation of the RAF-ERK signaling pathway by oncogenic mutations of B-RAF. Cell *116*, 855–867.

Workman, P. (2004). Combinatorial attack on multistep oncogenesis by inhibiting the Hsp90 molecular chaperone. Cancer Lett. *206*, 149–157.

Wriggers, W., Milligan, R.A., and McCammon, J.A. (1999). Situs: a package for docking crystal structures into low-resolution maps from electron microscopy. J. Struct. Biol. *125*, 185–195.

Xu, Y., and Lindquist, S. (1993). Heat-shock protein Hsp90 governs the activity of Pp60(V-Src) kinase. Proc. Natl. Acad. Sci. USA *90*, 7074–7078.

Xu, Y., Singer, M.A., and Lindquist, S. (1999). Maturation of the tyrosine kinase c-Src as a kinase and as a substrate depends on the molecular chaperone Hsp90. Proc. Natl. Acad. Sci. USA *96*, 109–114.

Xu, W., Mimnaugh, E., Rosser, M.F., Nicchitta, C., Marcu, M., Yarden, Y., and Neckers, L. (2001). Sensitivity of mature Erbb2 to geldanamycin is conferred by its kinase domain and is mediated by the chaperone protein Hsp90. J. Biol. Chem. *276*, 3702–3708.

Xu, W., Yuan, X., Xiang, Z., Mimnaugh, E., Marcu, M., and Neckers, L. (2005). Surface charge and hydrophobicity determine ErbB2 binding to the Hsp90 chaperone complex. Nat. Struct. Mol. Biol. *12*, 120–126.

Zhang, W., Hirshberg, M., McLaughlin, S.H., Lazar, G.A., Grossmann, J.G., Nielsen, P.R., Sobott, F., Robinson, C.V., Jackson, S.E., and Laue, E.D. (2004). Biochemical and structural studies of the interaction of Cdc37 with Hsp90. J. Mol. Biol. *340*, 891–907.

Zhao, Q., Boschelli, F., Caplan, A.J., and Arndt, K.T. (2004). Identification of a conserved sequence motif that promotes Cdc37 and cyclin D1 binding to Cdk4. J. Biol. Chem. *279*, 12560–12564.